International Journal of Plasticity xxx (xxxx) xxx–xxx

Contents lists available at ScienceDirect

International Journal of Plasticity

journal homepage: www.elsevier.com/locate/ijplas

On the origin of softening in the plastic deformation of metallic glasses

M. Zhang[a,b,*], Y. Chen[b,c], W. Li[a]

[a] Institute of Advanced Wear & Corrosion Resistant and Functional Materials, Jinan University, Guangzhou, 510632, China
[b] State Key Laboratory of Nonlinear Mechanics, Institute of Mechanics, Chinese Academy of Sciences, Beijing, 100190, China
[c] School of Engineering Sciences, University of Chinese Academy of Sciences, Beijing, 100049, China

ARTICLE INFO

Keywords:
Metallic glass
Softening
Nanoindentation
Structural relaxation

ABSTRACT

In the plastic deformation of amorphous materials, dilatation occurs universally with softening. However, the critical question that whether softening is caused by dilatation or not remains an ansatz and requires experimental examination. In this work, by examining the deformation behaviors of 3 metallic glasses (MGs) with distinct Johari-Goldstein (JG) relaxation characteristics before and after crystallization with nanoindentation, it is found that the origin of softening is probably not dilatation but the collective mode in the activation dynamics of shear transformation zones (STZs). Since the deformation in the creep stage of nanoindentation of the MGs originates from the "delayed plasticity" from the loading stage and depends on the softened deforming state of the MGs, the creep depth vs. time curves in the creep stage of nanoindentation of the MGs are examined and display similar loading rate dependent softening phenomena for both the glassy and crystallized MGs. The stretched exponent and relaxation time characterizing the deformation dynamics in the creep stage of nanoindentation are derived by fitting the creep depth *vs.* time curves with the Kohlrausch-Williams-Watts (KWW) equation. The stretched exponents indicate similar collective modes in the activation dynamics of the elementary deformation units (STZs in glassy MGs and dislocations in crystallized MGs). The relaxation times manifest similar softening effects in the deformation accommodation processes of both the glassy and crystallized MGs, except for a glassy La MG of which the relaxation time is extraordinary for its pronounced JG relaxation. The extraordinary relaxation time of the glassy La MG precludes the possibility of shear dilatation being the main cause for the softening of the glassy La MGs indicated by the loading rate dependent creep depth vs. time curves. The stretched exponent and the relaxation time indicate the homological softening dynamics in the plastic deformation of the glassy and crystallized MGs. For the distinct elementary deformation units, i.e., STZs in glassy MGs and dislocations in crystallized MGs, noting the absence of dilatation in dislocation movements, the softening phenomena in the plastic deformation of both the glassy and crystallized MGs is suggested to originate from the collective mode in the activation dynamics of the elementary deformation units, rather than from local properties of elementary deformation units, such as dilatation in STZs.

1. Introduction

Metallic glasses (MGs) are a new species of amorphous materials with unique disordered atomic structures (Cheng and Ma, 2011),

* Corresponding author. Institute of Advanced Wear & Corrosion Resistant and Functional Materials, Jinan University, Guangzhou, 510632, China.
E-mail address: m.zhangiwrm@jnu.edu.cn (M. Zhang).

https://doi.org/10.1016/j.ijplas.2018.12.004
Received 25 October 2018; Accepted 11 December 2018

which exhibits desirable mechanical properties (Hufnagel et al., 2016), biocompatibility (Li and Zheng, 2016), magnetic properties and catalytical properties (Wang, 2009). These features of MGs impart them with a broad prospect in industrial applications (Khan et al., 2018). Among the properties of MGs, the mechanical properties, specifically the plasticity (Wu et al., 2011, 2015), largely determines the applicability of MGs as engineering materials. Because of the catastrophic failure mode caused by the precipitation of highly localized shear band in plastic deformation (Chen et al., 2013; Jiang and Dai, 2009), the tensile plasticity of MGs has been under relentless pursuit (Ketov et al., 2015; Wang et al., 2017; Yu et al., 2012) up until nowadays. Hence, clarifying the plasticity mechanisms of MGs is imperative for their future application.

Since developed in the early 1990s, nanoindentation (Oliver and Pharr, 2010) has evolved into an extremely useful technique in examining the microscale mechanical properties of materials (Ma et al., 2012; Zhang and Ohmura, 2014), especially for the materials with limited ductility, like MGs (Chen and Lin, 2010; Yoo et al., 2012). This is because that the deformation on nanoscales delivers clean information on the underlying deformation mechanisms (Dahlberg et al., 2014; Jang et al., 2011; Xiao et al., 2017; Zhang et al., 2017a), and that the highly constrained conditions under the indenter guarantees a sustainable deformation mode for brittle materials, providing rich deformation phenomena. Strain-hardening exponent, fracture toughness, viscoelastic properties and creep parameters have been tentatively extracted from the data recorded in instrumental nanoindentation tests (Dean et al., 2010). The flow constitutive relation determined from the creep tests conducted under nanoindentation has been scaled to that determined from conventional creep tests (Ginder et al., 2018; Phani and Oliver, 2016). These results prove that nanoindentation is an effective technique in revealing the creep mechanisms of engineering materials (Gan and Tomar, 2010; Su et al., 2013; Zhang et al., 2017b). As nanoindentation creep is performed immediately following a loading stage during which the maximum creep load is reached at different loading rates, the loading rate-dependent creep behaviors of various materials are systematically characterized to understand their plasticity mechanisms (Lee et al., 2016; Liu et al., 2015; Tehrani et al., 2011; Wang et al., 2010, 2018b). Enlightened by the nanoindentation creep technique, since the deformation in the *creep* stage of normal nanoindentation with different loading rates adopted in the loading stage is believed to stem from the "delayed plasticity" from the loading stage of nanoindentation (Klaumünzer et al., 2011; Schuh et al., 2004; Schuh and Nieh, 2003), revealing the origin and the dynamics of the deformation in the *creep stage* of nanoindentation with different loading rates adopted in the loading stage should also bring out new understandings on the plasticity mechanisms of engineering materials.

In the plasticity mechanisms of MGs, shear dilatation occurs universally and concomitantly with softening which usually leads to a catastrophic failure (Spaepen, 1977), as having been systematically confirmed in the literature (Pan et al., 2011, 2018). However, the causality between dilatation and softening in the shear transformation zone (STZ)-based flow model (Argon, 1979; Spaepen, 1977) of amorphous materials remains an ansatz that the dilatation created locally in a previous STZ activation would facilitate the activation of subsequent STZs nearby, i.e., dilatation causes softening. This is because of the problem that it is difficult to experimentally prove that dilatation induces softening, since *the observation of softening is post-mortem where dilatation and softening are simultaneously observed*. Recently, model glasses in simulations (Patinet et al., 2016; Zylberg et al., 2017) and colloidal glasses (Lu et al., 2018) indicate that the activation of STZ does not depend on the initial free volume content at the site of the STZ and the free volume at the STZ site even does not exhibit a monotonous increase in the activation of an STZ. This observation suggests that the excess free volume created via *local* dilatation in previous STZ activation cannot facilitate subsequent STZ activation as assumed in the flow theory (Argon, 1979; Spaepen, 1977), i.e., dilatation may not induce softening. Not too long ago, Bhowmick et al. (2006) had reported a softening phenomenon in a Zr-based MG with reduced free volume concentration after deformation, i.e., not dilatation but "contraction". The reduced free volume is ascribed to the formation of nanovoids via the convergence of free volume. However, the existence of nanovoids is subtle to verify. Even if the existence of nanovoids could be verified (Wu et al., 2010), the problem mentioned above still exists. Via quantitative density measurement, Schmidt et al. (2015) found both densification and dilatation in the deformed MG, suggesting that dilatation might not be the only reason for softening. Therefore, a critical question arises as whether softening is caused by dilatation or not. If not, then what causes softening?

Previously, to reveal the plasticity mechanisms of MGs, the relationship between Johari-Goldstein (JG) relaxation and the loading rate-dependent serrated deformation in MGs have been interpreted with the relaxation time derived from the creep stage of nanoindentation (Zhang et al., 2016b). As a result, a loading rate-independent relaxation time for a La MG with pronounced JG relaxation is observed. Based on this relaxation time, pronounced JG relaxation is suggested to be able to suppress the local softening effect in the deformation accommodation process in the plastic deformation of MGs (Zhang et al., 2018) and thus be potentially able to improve the plasticity of MGs (Qiao et al., 2016). Therefore, the loading rate-dependent deformation in the creep stage of nanoindentation is of particular interests to understanding the softening mechanism in MGs. What's more, as mentioned above, the creep stage of nanoindentation characterizes the "delayed plasticity" of materials being plastically deformed underneath the indenter, and thus depends intimately on the softened deforming state of the MGs in the loading stage, providing a critical resort to examining "quasi in-situ" the softening effect in the plastic deformation of MGs, unlike the post-mortem tests having been done previously (Pan et al., 2018). For the complicated stress state under the indenter and utilizing the absence of dilatation in crystalline structures, a systematic study on the MGs before and after crystallization is necessary to thoroughly understand the plastic deformation of MGs in nanoindentation (Burgess and Ferry, 2009; Castellero et al., 2008; Kramer et al., 2018; Wang et al., 2018b; Yang et al., 2016b).

For the complex composition of MGs which is critical for their glass forming ability (Cheng and Ma, 2011), to gain an overall view on the plastic deformation behaviors of MGs before and after crystallization, different types of MGs are needed for the current study. Due to the characteristic-less feature of amorphous structure, MGs with distinct JG relaxation characteristics are selected (Yu et al., 2014), noting the crucial role of JG relaxation in the plastic deformation of MGs (Zhang et al., 2018). Therefore, nanoindentation with different loading rates adopted in the loading stage are performed on 3 MGs with distinct JG relaxation characteristics (i.e., La ($La_{62}Al_{14}Ag_{2.34}Ni_{10.83}Co_{10.83}$) with pronounced JG relaxation, Pd ($Pd_{40}Cu_{30}Ni_{10}P_{20}$) with less pronounced JG relaxation, and Zr

($Zr_{41.2}Ti_{13.8}Cu_{12.5}Ni_{10}Be_{22.5}$) with no pronounced JG relaxation) in both glassy and crystallized states. By examining the deformation in the creep stage of nanoindentation, it is found that the MGs in both glassy and crystallized states show similar softening phenomena. The stretched exponent and relaxation time characterizing the deformation dynamics in the creep stage of nanoindentation are derived with the Kohlrausch-Williams-Watts (KWW) equation. With increasing loading rates adopted in the loading stage, the decreasing stretched exponents suggest similar collective modes in the deformation dynamics of the glassy and crystallized MGs, and the decreasing relaxation times manifest similar softening effects in the deformation accommodation process of the glassy and crystallized MGs, except for the glassy La MG of which an extraordinary nearly constant relaxation time is observed for its pronounced JG relaxation. This nearly constant relaxation time precludes the possibility of shear dilatation being the main cause for the softening of the glassy MGs, supports the crucial role of JG relaxation in the plasticity of MGs (Qiao and Pelletier, 2014), and provides an important clue to pin on the origin of JG relaxation in MGs. For the distinct elementary deformation units, i.e., STZs in glassy MGs and dislocations in crystallized MGs, the collective mode in the deformation dynamics of the glassy and crystallized MGs, instead of local properties of elementary deformation units like dilatation in STZs, is probably the main cause for the softening phenomena.

2. Experimental procedure

$Zr_{41.2}Ti_{13.8}Cu_{12.5}Ni_{10}Be_{22.5}$, $La_{62}Al_{14}Ag_{2.34}Ni_{10.83}Co_{10.83}$, and $Pd_{40}Cu_{30}Ni_{10}P_{20}$ MGs (at.%) in the form of plates of a size of 2 mm × 30 mm × 40 mm are prepared by copper mould casting under a Ti-gettered Ar atmosphere from master alloys. Amorphous structures of the prepared alloys are verified by X-ray Diffraction (XRD, Smartlab-9) and differential scanning calorimeter (DSC, Netzsch DSC STZ 449 F3). The crystallized MG samples are obtained by heating the MGs to a temperature (La: 360 °C, Pd: 420 °C, Zr: 550 °C) above their respective crystallization exothermal peak to guarantee crystallization is fully completed, and maintaining the temperature for 1 min. The crystallized structure of the 3 MGs after thermal treatment are also verified by the X-ray diffraction. The JG relaxation of the MGs in both glassy and crystallized states are examined with a Dynamical Mechanical Analyzer (TA, DMA Q800). Before nanoindentation, the samples were carefully polished to a mirror finish. Nanoindentation is conducted on an Agilent G200 Nanoindenter with a Berkovich diamond tip at room temperature (RT = 298 K). The ratios $T_r = RT/T_g$ for the glassy MGs are as follows: La (T_g = 445 K, T_r = 0.67), Zr (T_g = 633 K, T_r = 0.47), Pd (T_g = 572 K, T_r = 0.52), where T_g is the glass transition temperature. Load control mode and a group of loading rates $\dot{P}$: 0.33 mN/s, 1.32 mN/s, 13.2 mN/s, and 70 mN/s are selected. The test is composed by: loading to a maximum load P_{max} of 200 mN at a constant loading rate; maintaining the load for 10 s at P_{max}; unloading to 10% of P_{max} at a rate of 10 mN/s; holding the load for 10 s for thermal drift calibration, and unloading completely. To guarantee the reliability of the results, each test is repeated 7 times. To reduce the effects of thermal drift (Maier et al., 2013) and to exclude the long time creep deformation effect, a reasonable dwell period of 10s for the creep stage of nanoindentation is selected, because which is usually adopted in nanoindentation for the materials under the indenter to reach a steady mechanical state (Wei et al., 2007).

3. Results

To confirm the crystalline structures of the crystallized MGs, Fig. 1(a)-(c) show the XRD patterns of the La, Pd, and Zr MGs in both glassy and crystallized states, respectively. It can be seen that the 3 crystallized MGs show clear Bragg diffraction peaks indicating their fully crystalline structures, but the 3 glassy MGs show only a diffusive “hump” indicating their monolithic amorphous structures. The XRD patterns of the crystallized MGs exhibit multiple diffraction peaks, indicating the complexity of the compositions of MGs. Thus, to systematically understand the plastic deformation behaviors of MGs after crystallization, 3 MGs with different JG relaxation characteristics are examined.

Fig. 2 shows the reduced modulus and hardness of the 3 MGs in both glassy and crystallized states. As previously observed (Afonin et al., 2016), both reduced modulus and hardness increase for the 3 MGs after crystallization. With the hardness, the flow stress of the 3 crystallized MGs beneath the indenter can be estimated as (Schuh and Nieh, 2004): $\sigma = H/3$. The flow stresses of the 3 crystallized MGs in nanoindentation are averagely ~1.3 GPa for La MG, ~2.6 GPa for Pd MG, ~4.1 GPa for Zr MG. Based on the flow stresses, the obstacle-limited dislocation nucleation is inferred to be the dominant deformation mechanism (Gerberich et al., 1995) of the crystallized MGs. Most importantly, it is noted that the small error bars of the hardness and modulus suggests the homogeneous mechanical performances of the crystallized MGs and supports the feasibility of comparing the nanoindentation behaviors of MGs before and after crystallization.

Since the creep stage of nanoindentation immediately follows the loading stage, the deformation in the creep stage depends intimately on the softened deforming state of the MGs in the loading stage. To examine the deforming state of the MGs, Fig. 3 (a)-(c) show the typical load (P) *vs*. displacement (h) curves of the 3 crystallized MGs and Fig. 3 (d)-(f) show the P-h curves of the 3 glassy MGs, under different loading rates. For clarity, the curves are properly shifted along the transversal coordinates. Generally, the crystallized MGs and the glassy MGs exhibit similar P-h curves. By closer examination, it can be seen in Fig. 3 (b) that the P-h curves of the crystallized Pd MG exhibit moderate “pop-in” events or serrations. Upon increasing loading rates, the serrations decays rapidly and become indiscernible. However, in Fig. 3 (a) and (c), both the crystallized La and Zr MGs display no serrations. For the glassy MGs, in Fig. 3 (e), prominent serrations can be found for the glassy Pd MG (Schuh et al., 2002). In comparison, the glassy Zr MG (Fig. 3(f)) shows much slighter serrations and the glassy La MG (Fig. 3(d)) shows no obvious serrations. Upon increasing loading rates, the serrations of the glassy Pd and Zr MGs also decay rapidly.

To clearly examine the evolution characteristics of the serrations under increasing loading rates, the raw P-h curves are subtracted by their power law fits (Sneddon, 1965): $P = Ch^m$, where C is a constant; m is the power index. The Δh-P curve, i.e. Δh at the same load P, is the difference between the P-h curve and its power law fit. As shown in Fig. 4 (a) and (c), the crystallized La and Zr MGs

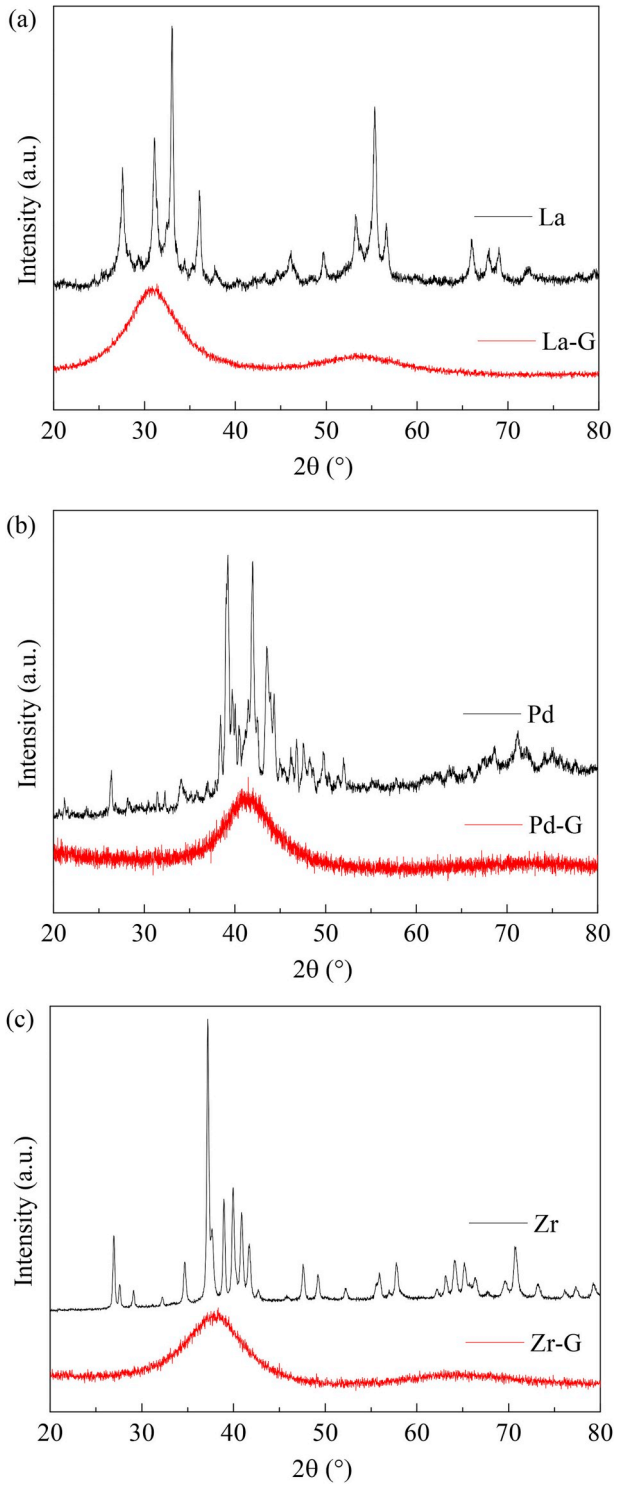

Fig. 1. (Color online) XRD patterns of the La (a), Pd(b), and Zr(c) metallic glasses (MGs) in crystallized state and in glassy state. "La-G" stands for the glassy La MG and so on. (For interpretation of the references to color in this figure legend, the reader is referred to the Web version of this article.)

exhibit a group of smooth Δh-P curves, while the crystallized Pd MG exhibits a group of Δh-P curves with prominent serrations. The serrations on the Δh-P curves of the crystallized Pd MG also decays with increasing loading rates. These results are consistent with the P-h curves in Fig. 3(a)-(c). Interestingly, as shown in Fig. 4 (d)-(f), prominent serrations are shown on the Δh-P curves of all the 3 glassy MGs. Especially for the glassy La MG, the raw P-h curves show no serrations, but the Δh-P curves show clear serrations.

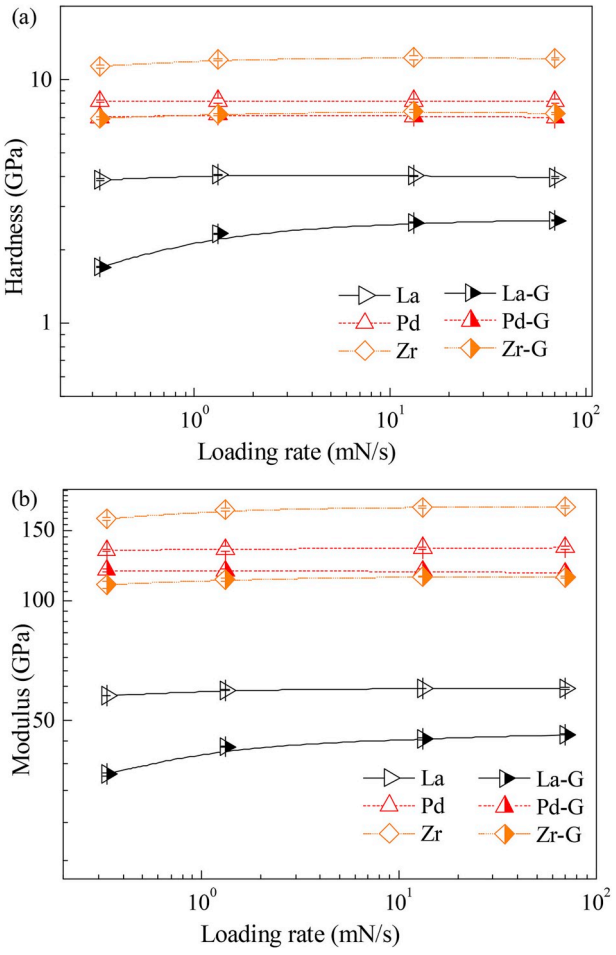

Fig. 2. (Color online) Hardness (b) and reduced modulus (a) of La, Pd, and Zr metallic glasses (MGs) in crystallized (open symbols) state and in glassy (half-solid symbols) state. It is noted that the error bar is too small and covered by the symbols of the data. "La-G" stands for the glassy La MG and so on. (For interpretation of the references to color in this figure legend, the reader is referred to the Web version of this article.)

Moreover, the serrations of the glassy La MG (Fig. 4(d)) increase with increasing loading rates, rather than decay like the glassy Pd and Zr MGs (Fig. 4(e) and (f)), providing more information on the serrations and suggesting the importance of examining serrations with the Δh-P curves. As will be shown later, the serrations observed could be well explained with the relaxation times derived from the creep stage of nanoindentation (Zhang et al., 2016b).

Fig. 5(a)-(c) show the creep depth *vs*. time curves of the crystallized La, Pd, and Zr MGs in the creep stage of nanoindentation with different loading rates adopted in the loading stage. Fig. 5(d)-(f) show the creep depth *vs*. time curves of the 3 MGs in glassy state. The solid points are experimental results and the solid lines are the numerical fits. For comparison, the scales of the coordinates in Fig. 5 are set as the same for each MG in both glassy and crystallized states. It is noted that the creep depth here does not refers to the "real" creep deformation in nanoindentation creep, but originates from the "delayed plasticity" from the loading stage. It is also important to note that with increasing loading rate, the creep depth increases for all the 3 MGs in both glassy and crystallized states, indicating similar loading rate dependent softening phenomena in plastic deformation. For example, under a loading rate of 0.33 mN/s, the creep depth is only on the order of 1 nm, while under a loading rate of 70 mN/s, the creep depth is on the order of 10 nm, indicating a prominent softening effect and the effectiveness of the creep stage of nanoindentation in characterizing the "delayed plasticity" of MGs. To understand the deformation dynamics, the creep depth *vs*. time curves are fitted with the Kohlrausch-Williams-Watts (KWW) equation (Williams and Watts, 1970): $h_c = h_0(1 - \exp(-(t/\tau_c)^{\beta}))$, where h_c is the time-dependent creep depth; h_0 is the creep depth limit, τ_c is a relaxation time characterizing the release rate of the "delayed plasticity", and β is a stretched exponent indicating the deviation of the deforming process from the exponential process. Since either the dislocations nucleation dominated deformation in crystallized MGs or the STZ dominated deformation in glassy MGs is a thermally activated process, all the experimental results exhibit good agreements with the KWW fits (Zhang et al., 2016b).

Fig. 6 (a) and (b) show the stretched exponent β and the relaxation time τ_c of the glassy and crystallized La, Pd, and Zr MGs. The lines are drawn as eye guides. Firstly, it can be seen in Fig. 6(a) that the β of the 3 MGs in both glassy and crystallized states decrease concordantly from $\sim$1.5 to $\sim$0.3 with increasing loading rate. It is noted that the relatively higher value of β of roughly 1.5 at the

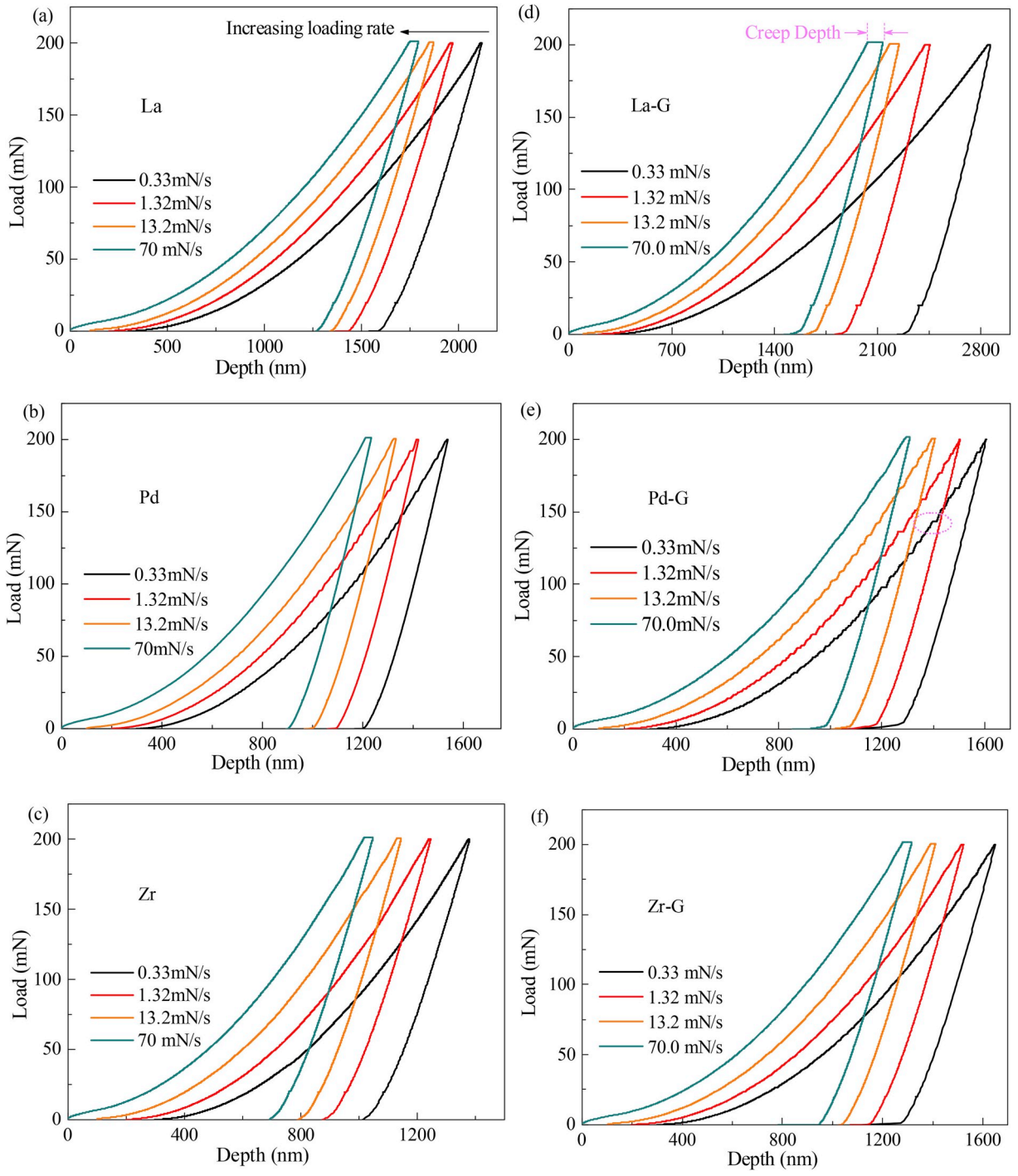

Fig. 3. (Color online) The load *vs*. displacement curves at different loading rates for La (a), Pd (b), and Zr (c) metallic glasses (MGs) in crystallized state and for La (d), Pd (e), and Zr (f) MGs in glassy state. "La-G" stands for the glassy La MG and so on. (For interpretation of the references to color in this figure legend, the reader is referred to the Web version of this article.)

lowest loading rate indicates a compressed relaxation process of the deformation in the creep stage of nanoindentation. This result is consistent with various observations made in different MGs with distinct methods (Luttich et al., 2018), supporting the reliability of the current results. Under increasing loading rate, the decreasing β indicates a stretched-exponentially increasing behavior of the creep depth, and suggests that the activation energies of the elementary deformation units of the 3 MGs in both crystallized and glassy states become non-uniform and follow a broader distribution (Wang et al., 2014). The concordantly decreasing β thus suggests that

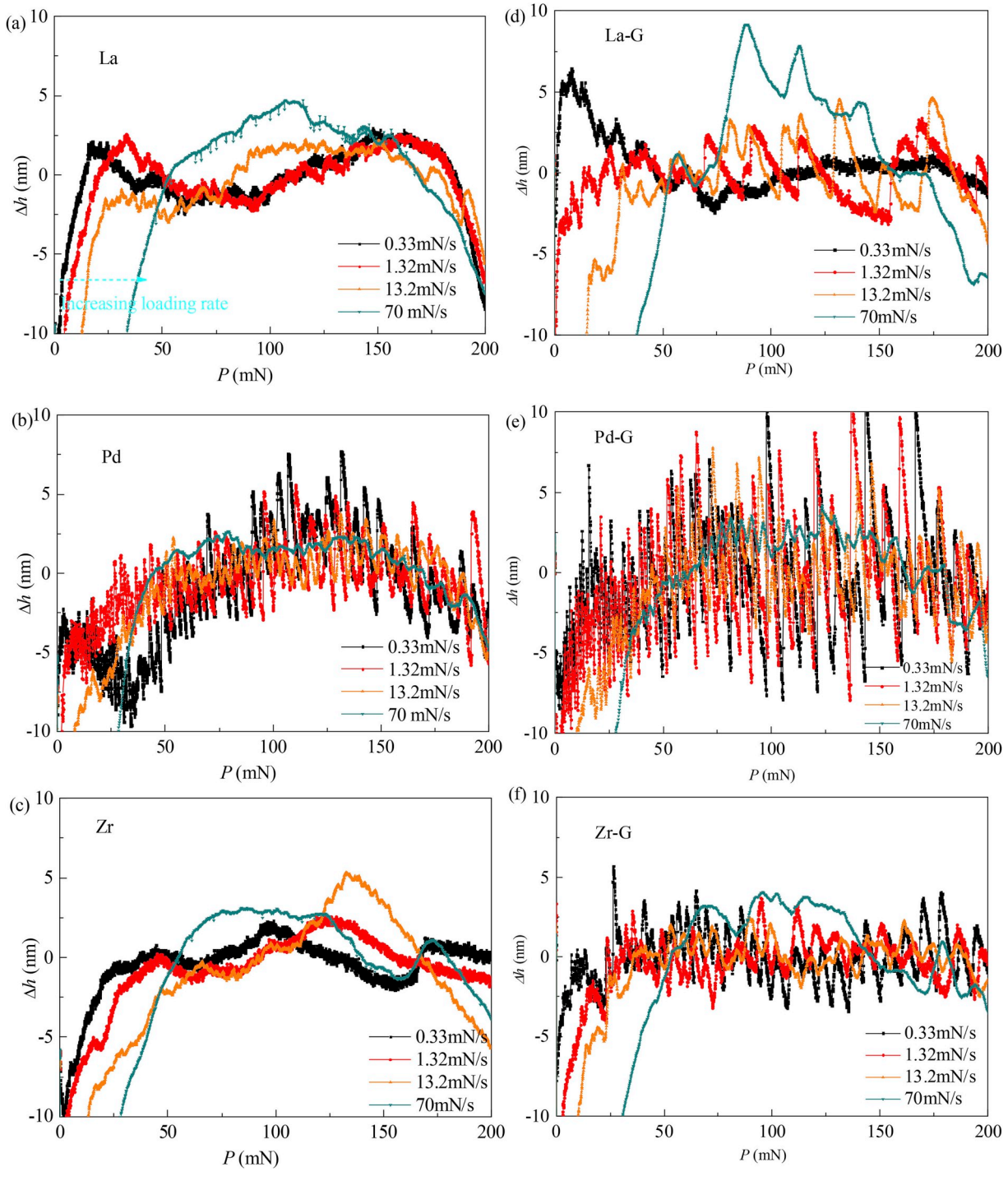

Fig. 4. (Color online) Serrations of the La, Pd, and Zr metallic glasses (MGs) at different loading rates for La (a), Pd (b), and Zr (c) MGs in crystallized state and for La (d), Pd (e), and Zr (f) MGs in glassy state. "La-G" stands for the glassy La MG and so on. (For interpretation of the references to color in this figure legend, the reader is referred to the Web version of this article.)

the activation dynamics of dislocations (in crystallized MGs) and STZs (in glassy MGs) of 3 MGs follows similar evolution upon increasing loading rate. Secondly, as shown in Fig. 6(b), the relaxation time τ_c of Pd and Zr MGs in both glassy and crystallized states decrease similarly and monotonously from ~10s to ~0.1s, manifesting a softening phenomenon in alignment with Fig. 5. However, τ_c of the glassy La MG remains around ~10s, i.e., exhibiting no softening effect, in contrast to the softening phenomenon in Fig. 5 (d). Intriguingly, τ_c of the crystallized La MG exhibits a decreasing tendency similar to the Pd and Zr MGs in both glassy crystallized states,

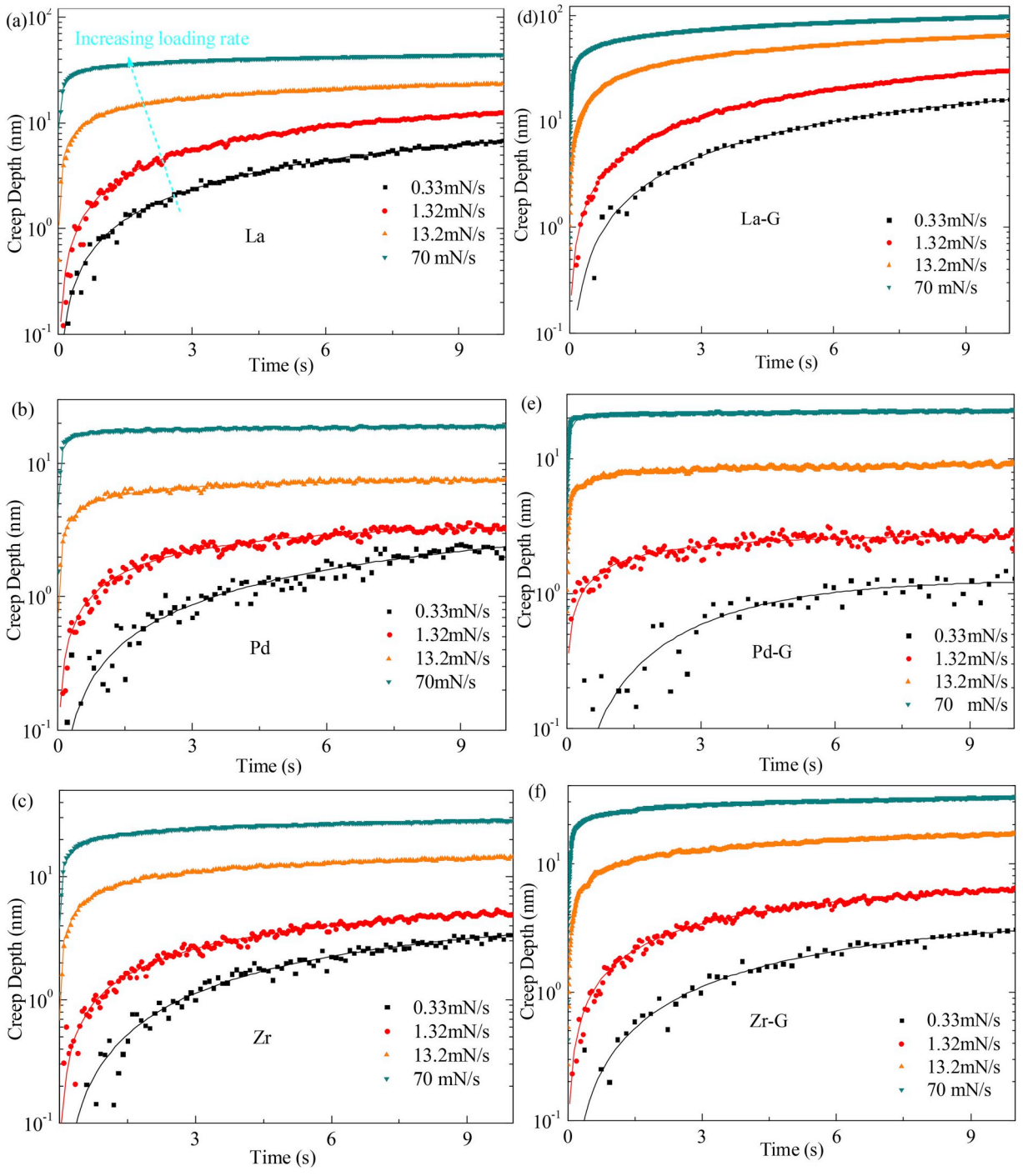

Fig. 5. (Color online) Creep depth *vs*. time curves of metallic glasses (MGs) in the creep stage of nanoindentation with the maximum load reached at different loading rates for La (a), Pd (b), and Zr (c) MGs in crystallized state and for La (d), Pd (e), and Zr (f) MGs in glassy state. Solid lines are the Kohlrausch–Williams–Watts (KWW) equation fits. "La-G" stands for the glassy La MG and so on. (For interpretation of the references to color in this figure legend, the reader is referred to the Web version of this article.)

i.e., a similar softening phenomenon. Therefore, although similar softening phenomena in Fig. 5 and activation dynamics in Fig. 6(a) are displayed, an extraordinary τ_c is observed for the glassy La MG. As having been observed in amorphous selenium (Su et al., 2010), the deformation mode of the glassy MGs under nanoindentation exhibits a close dependence on temperature. To examine the effect of temperature on the deformation of the 3 glassy MGs, as shown in **Part 2**, the reduced temperature $T_r = \mathrm{RT}/T_g$ of the 3 MGs are calculated: La ($T_g = 445$ K, $T_r = 0.67$), Zr ($T_g = 633$ K, $T_r = 0.47$), Pd ($T_g = 572$ K, $T_r = 0.52$). Thus, the deformation of the 3 glassy

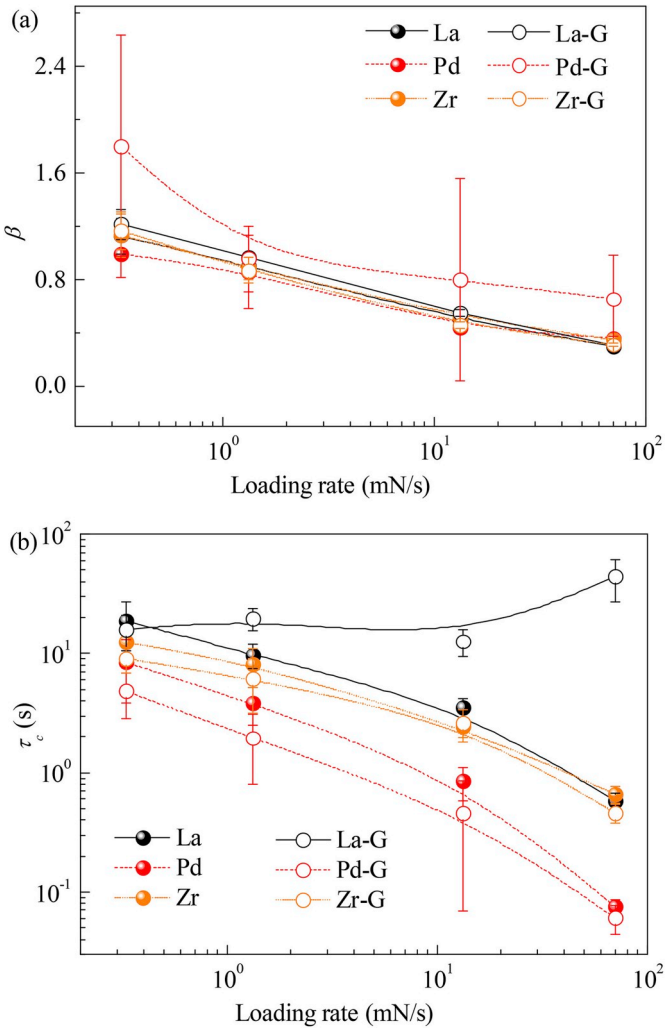

Fig. 6. (Color online) Stretched exponent β (a) and relaxation time τ_c (b) of the crystallized (solid circles) and glassy (open circles) La, Zr, and Pd metallic glasses (MGs) fitted from the creep depth *vs.* time curves of in the creep stage of nanoindentation. "La-G" stands for the glassy La MG and so on. (For interpretation of the references to color in this figure legend, the reader is referred to the Web version of this article.)

MGs are concluded to be dominated by shear bands (Schuh et al., 2004). More works on different La MGs and other MGs systems (such as Mg, Ce, etc.) confirms that τ_c depends intimately on the MG systems, and the extraordinary τ_c of the glassy La MG is not due to its relatively high $T_r = 0.67$. As will be explained later, τ_c characterizes the deformation accommodation rate in the plastic deformation of the MGs and the extraordinary τ_c of the glassy La MG is due to its pronounced JG relaxation (Yu et al., 2014).

4. Discussion

4.1. Origin of the deformation in the creep stage of nanoindentation

As stated before, the deforming state of MGs in the loading stage of nanoindentation as shown in Figs. 3 and 4 determines the deformation dynamics in the creep stage, i.e., the softening phenomenon observed in Figs. 5 and 6, indicated by the creep depth, the stretched exponent and the relaxation time. As proposed in (Schuh and Nieh, 2003), in the plastic deformation of MGs, the activated STZs automatically assemble into shear bands (Sopu et al., 2017). Under low loading rates, one single shear band can rapidly operate and accommodate the applied deformation via *relaxation* (Murali et al., 2007), leading to a displacement "pop-in" or a serration. A typical "pop-in" extracted from Fig. 2 (e) marked with an ellipse is shown in Fig. 7. The displacement jumps forward rapidly. However, at loading rates exceeding the rate of *relaxation* via a single shear band, multiple shear bands form to accommodate the applied deformation. In this scenario, a virtual "field" of shear bands continuously operate and accommodate the imposed deformation and smear out the serrations, as shown in Fig. 4(e) and (f). For the crystallized MGs, dislocations instead of shear bands accommodate the deformation (Wang et al., 2018a; Zhang and Ohmura, 2014) and analog explanation applies. Therefore, the

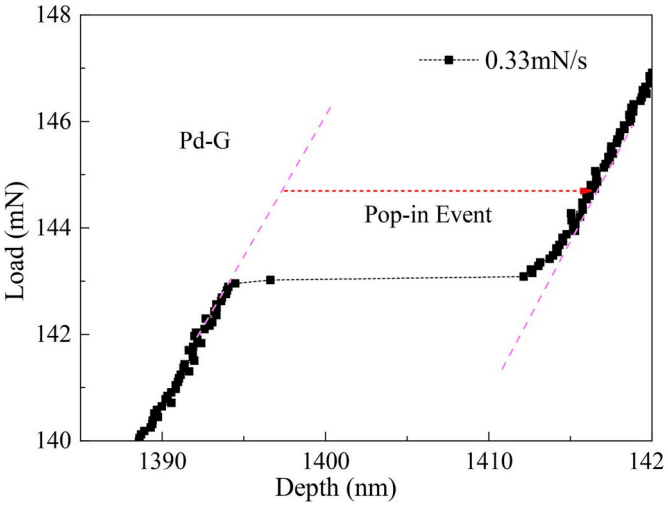

Fig. 7. (Color online) A typical pop-in event on the load-displacement curve. The data points are recorded at a frequency of 5 Hz. The sparse data points indicates the transient nature of the pop-in event. "Pd-G" stands for the glassy Pd metallic glass (MG). (For interpretation of the references to color in this figure legend, the reader is referred to the Web version of this article.)

deformation accommodation process which determines the deforming state of MGs is crucial to elucidate the origin of the deformation in the creep stage of nanoindentation.

To illustrate the deformation accommodation process, as shown in Fig. 8, the serrations of MGs can be understood as a stick-slip process (Klaumünzer et al., 2011). When the critical yield point **A** is approached as shown in Fig. 8(a), (c) and (d), the anelastic deformation accumulated during the loading stage will partly transit into plastic deformation via *relaxation* in shear bands, leading to a serration. As shown in Fig. 8(b), a serration indicates that the MGs transit from a high potential energy state **A** to a low potential energy state **B** (Klaumünzer et al., 2011). For the load-control mode in nanoindentation, a displacement "pop-in" under constant load is observed as shown in Fig. 7. Therefore, the deformation accommodation process refers to the transition from anelasticity to

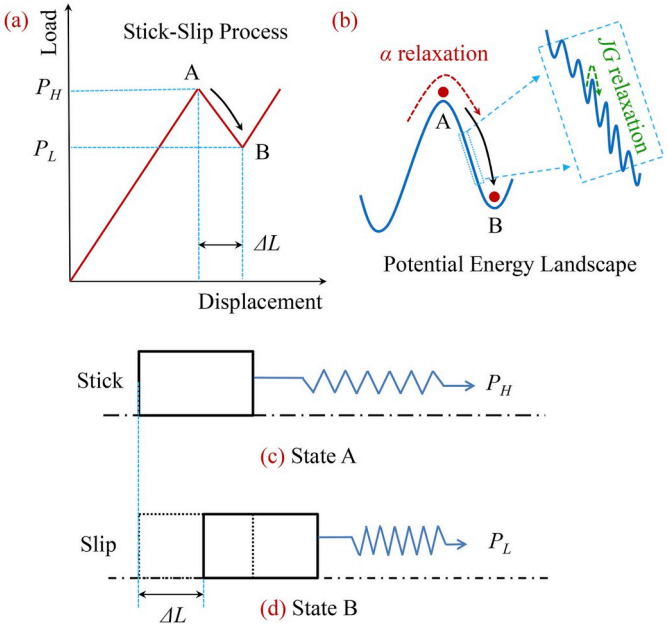

Fig. 8. (Color online) illustration of the serration with the Stick-Slip process. (a) a load-displacement curve with a serration: **A** indicates the stick state; **B** indicates the slip state (b) a potential energy landscape view on the strain accommodation process in a serration. For glassy metallic glasses (MGs), α relaxation composed by Johari-Goldstein (JG) relaxations corresponding to the yield and plastic deformation; the closeup shows the JG relaxation which corresponds to the anelastic deformation; (c) stick state; (d) slip state. It is noted here that, due to the confined deformation mode of nanoindentation, a constant load rather than a drop of load is observed in the "pop-in" event. (For interpretation of the references to color in this figure legend, the reader is referred to the Web version of this article.)

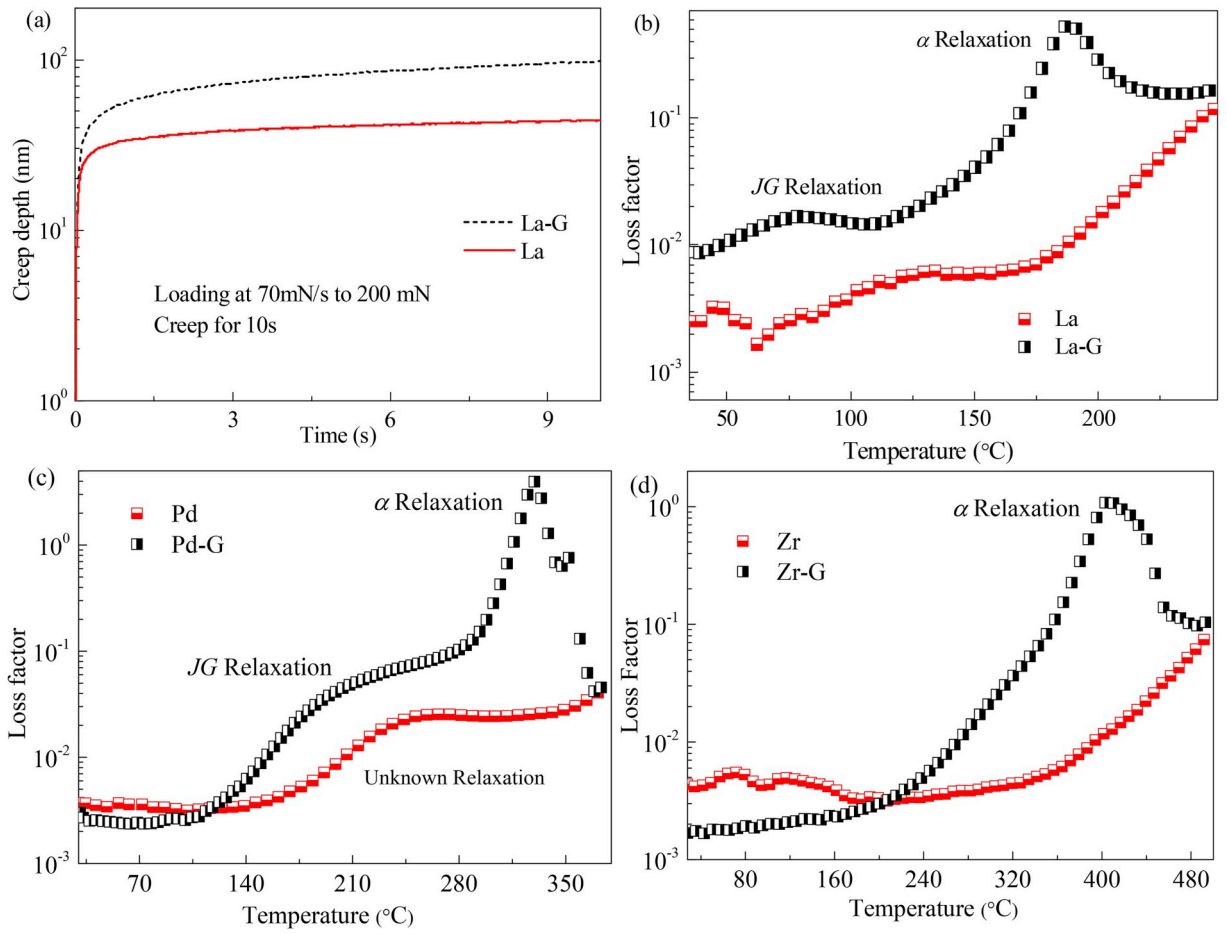

Fig. 9. (Color online) Typical creep depth vs. time curves for the La metallic glass (MG) in crystallized state and in glassy state (a). The loss factor of the La(b), Pd(c), and Zr(d) MGs in crystallized state and in glassy state measured by dynamic mechanical analyzer. "La-G" stands for the glassy La MG and so on. Noting that the logarithmic-linear plot is used for the loss factor. (For interpretation of the references to color in this figure legend, the reader is referred to the Web version of this article.)

plasticity, i.e., the anelastic deformation stored in the MGs underneath the indenter transits into plastic deformation, via *a relaxation process of STZ operations inside shear bands*. The abrupt transition from accumulated anelasticity to plasticity, i.e., "delayed plasticity", leads to "pop-in".

Noting the "pop-in" in Fig. 7 during which the deformation occurs at a constant load, the creep stage of nanoindentation can be viewed as a *purposely designed* "pop-in". The deformation in the creep stage should also stem from the "delayed plasticity" and the relaxation time τ_c indicates the average deformation accommodation rate in the plastic deformation of the glassy and crystallized MGs (Selyutina et al., 2016), i.e., *the rate of dislocation movements or STZ operations*. Based on the physical meaning of τ_c, the serrations observed in Fig. 4 can be explained as follows. As shown in Fig. 6(b), τ_c decreases with increasing loading rate, which enhances the anelasticity to plasticity transition rate, mitigates the accumulated anelastic deformation, and reduces the size of serrations shown in Fig. 4, except for the glassy La MG, of which the nearly constant τ_c explains the increasing serrations in Fig. 4(d), for the insufficient anelasticity to plasticity transition rate at increasing loading rates. With these concepts, we will address the deformation dynamics of the MGs in the creep stage of nanoindentation in the following content of this section.

4.2. Relaxation times of the MGs in glassy and crystallized states

As shown in Fig. 6(b), the glassy La MG shows a nearly constant relaxation time τ_c, while the crystallized La MG displays a decreasing relaxation time τ_c similar to the Pd and Zr MGs in both glassy and crystallized states. Based on the explanation in **Part 4.1**, the decreasing τ_c actually indicates an increasing accommodation rate, i.e., a softening effect, in the deformation accommodation process. Fig. 9 (a) shows typical creep depth *vs.* time curves of the glassy and crystallized La MGs, with a loading rate of 70 mN/s in the loading stage. It can be seen that the creep depth of the crystallized La MG assumes its steady value much faster than the glassy La MG. It is noted that the creep depth in Fig. 5 indicates the total amount of softening effect, while the relaxation time indicates how fast can the total amount of softening could be reached via movements of elementary deformation units.

The deformation accommodation process is important to understand the constant τ_c of the glassy La MG. As shown in Fig. 8(b), on the potential energy landscape, the plastic deformation of MGs can be viewed as a stress-driven α relaxation process (Harmon et al., 2007), i.e., an assembly of JG relaxation processes (see Fig. 8 (b), a closeup view) which can be viewed as local reversible atomic rearrangements. According to the stick-slip model, the deformation accommodation process in the glassy MGs is the stage where the MG system explores neighborhood potential energy minimum via JG relaxations (i.e., the stage from state **A** to state **B**). Thus, τ_c of the glassy MGs is determined by JG relaxations. Noting the intrinsic softening nature of MGs, the constant τ_c of the glassy La MG exhibiting no softening effect is probably determined by its pronounced JG relaxation, compared to the Pd and Zr MGs as shown in Fig. 9. Therefore, τ_c of the glassy MGs should reflect the characteristic time scale of JG relaxations in plastic deformation. Noting that STZs have proved to be stress driven-JG relaxations (Harmon et al., 2007; Yu et al., 2014), τ_c of the glassy MGs also indicate the operation rate of the STZs. This is consistent with the discussion in **Part 4.1**. Therefore, the constant τ_c of the glassy La MG suggests that pronounced JG relaxation is able to suppress the softening effect in the operation of STZs (Zhang et al., 2018).

The decreasing τ_c of the Pd and Zr MGs in glassy state is thus attributed to their less-pronounced JG relaxations and the decreasing τ_c of the crystallized La MG is probably due to the absence of pronounced JG relaxation after crystallization. To confirm this point, Fig. 9(b)-(d) show the dynamic mechanical spectroscopies of the 3 MGs in both glassy and crystallized states. Compared to the glassy MGs, the crystallized MGs show no $\boldsymbol{\alpha}$ relaxation. The crystallized La MG shows no relaxation peak in the temperature range where JG relaxation exists for the glassy La MG. This result confirms that crystallization eliminates the JG relaxation in the crystallized La MG and supports that the nearly constant relaxation time of the glassy La MG is because of its pronounced JG relaxation. More works on La MGs with different JG relaxation characteristics also support this proposition and support the crucial role of JG relaxation in the plasticity of MGs (Qiao and Pelletier, 2014). It is also noted that the crystallized Pd MG exhibits an unknown relaxation much similar to the JG relaxation of the glassy Pd MG, which is worth further investigation. To further understand the correlation between JG relaxation and τ_c of MGs, more works are required in future.

It is noted that the decreasing τ_c of the glassy Pd and Zr MGs indicate the softening effect in the operation of STZs, while the constant τ_c of the glassy La MG suggests a non-softening effect in the operation of STZs. Recalling the similar softening phenomena in Fig. 5 exhibited by the loading rate dependent creep depth vs. time curves of the 3 glassy MGs, the constant τ_c of the glassy La MG suggests that the softening effect in the plastic deformation of the glassy MGs is not caused by the softening effect in the operation of STZs. However, as established in the STZ model (Argon, 1979; Spaepen, 1977), dilatation is locally created via the operation of STZ and assumed to subsequently induce a local softening effect in the operations of STZs. Hence, the constant τ_c of the glassy La MG might preclude the possibility of shear dilatation being the main cause for the softening in the plastic deformation of glassy MGs.

4.3. Homological softening dynamics in the glassy and crystallized MGs

It is attractive to note that the crystallized MGs exhibit similar softening behaviors to the glassy MGs, as indicated by the creep depth vs. time curves in Fig. 5 and the stretched exponent β and the relaxation time in Fig. 6. Similar softening phenomenon in crystalline materials has also been widely reported in Mg (Haghshenas et al., 2018), copper (Chen et al., 2016), and high entropy alloys (Zhang et al., 2016a) etc. As stated in **Part 3**, due to the high flow stress and the constrained deformation mode in nanoindentation, the emission of dislocations from the interface between the indenter and sample surface, i.e., the obstacle-limited dislocation nucleation, is inferred to be the dominant deformation mechanism (Gerberich et al., 1995) in the crystallized MGs.

To understand the similar softening behaviors, it is important to note that though dislocations and STZs are distinct elementary deformation units, the stress-driven temperature-assisted activation dynamics of these units obeys the universal enthalpy-entropy compensation rule. The compensation rule of the activation entropy stems from the multiple-excitation effect in the activation dynamics of dislocations (Wang et al., 2013) and STZs (Wang et al., 2015). As shown in Fig. 10, the multiple-excitation effect induced collective mode in the activation of dislocations (Fig. 10(a)) and STZs (Fig. 10(b)) (i.e., by combining an increasing number of dislocations or STZs to conquer higher activation energy barrier under higher loading rates) would lead to a broad distribution of the activation energy for an effective local deformation event (a cluster of dislocations or STZs of different numbers operate synchronically composing an effective local deformation event). The multiplication effect in the nanoindentation of MGs have also been confirmed by Schuh et al. (Schuh et al., 2004), where the nucleation dynamics of shear bands is emphasized. Thus, the distribution of activation energy requires that the dislocation nucleation dominated deformation dynamics of the crystallized MGs should exhibit a stretched-exponential form homological to that of the STZs dominated deformation dynamics of the glassy MGs, as evidenced by the concordantly decreasing stretched exponent shown in Fig. 6 (a). Thus, the homological activation dynamics of dislocations and STZs indicated by the stretched exponent and the relaxation time will lead to the similar softening behaviors of the MGs in both glassy and crystallized states.

Since the extraordinary relaxation time of the glassy La MG precludes the possibility of dilatation in STZ operations as the main cause for softening, for the distinct elementary deformation units, noting the absence of dilatation in dislocation movements, it is inferred that the softening effect observed in Fig. 5 is probably resulted from the collective mode in the activation dynamics of elementary deformation units rather than from the local properties of elementary deformation units, like shear dilatation in STZs. This conclusion is supported by observations in colloidal glasses (Lu et al., 2018) where the activation of STZ do not depend on the initial free volume content at the site of the STZ, indicating that the dilatation created locally after the operation of STZ cannot facilitate neighboring STZs and induces no softening effect. Sopu et al. (2017) found that the materials surrounding the activated STZ with lower dilatation but higher rotation would transmit the structural distortion of the activated STZ towards neighboring STZs. The rotation field on the materials surrounding the activated STZ would induce an asymmetric strain field on the neighboring STZs and facilitate their activation. The transmission effect of the materials surrounding STZ with lower dilatation but higher rotation

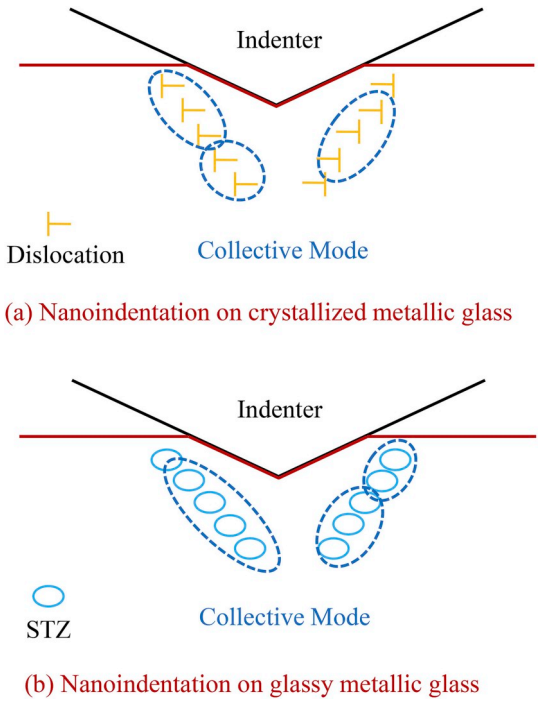

Fig. 10. (color online) The defects-mediated deformation kinetics for the glassy metallic glasses (MGs) and the crystallized MGs. (a) deformation in the creep stage of nanoindentation on the crystallized MGs; (b) deformation in the creep stage of nanoindentation on the glassy MGs. The ellipse indicates that the defects operate in a collective mode, i.e., operates synchronically.

resembles the long-range effect (i.e., collective effect) caused by the activation of STZ., i.e., the collective mode in the activation of STZ induces the softening effect (Sopu et al., 2017). Most recently, the softening of MGs is related to the softening of phonon spectra (Jiang et al., 2017; Mahjoub et al., 2016) where the collective mode of atom diffusion is involved. Chattoraj and Lemaitre (2013) also found that the softening effect coincides with the emergence of the correlations between STZs. This is probably why strong correlations between free volume-based “soft spots” and STZs could not be observed (Ding et al., 2016; Lu et al., 2018; Patinet et al., 2016; Yang et al., 2016a). Similar long-range stress effect also applies to the softening effect in the collective activation of dislocations (Wang et al., 2018a; Zaiser and Hahner, 1997). Actually, phenomenological flow models which take into account the collective effect in the plastic deformation of MGs and crystalline materials have already been established (Zaiser and Hahner, 1997; Zhang et al., 2013). By incorporating the collective effect, the strain rate softening phenomenon in the plastic deformation of both crystalline and amorphous materials can be predicted. These works also suggest the crucial role of the collective mode in the softening in the plastic deformation of engineering materials. Therefore, although indirectly, Fig. 6 provides an experimental proof for the observations made in simulations and model glasses that softening is probably not caused by dilatation, even though dilatation is critical in the yield of amorphous materials (Fornell et al., 2009). Our work implies an entropic origin of the softening effect and present alternative understandings on the defect-mediated plastic deformation in solid materials.

4.4. A kinematic perspective on the softening effect

From a kinematic perspective, the loading-rate dependent creep depth in crystalline materials, i.e., the softening effect, is often attributed to the restricted time scale available for dislocations to move on the slip planes, as suggested in (Haghshenas et al., 2018). In the loading stage, dislocations nucleate and move on the slip planes to accommodate the plastic deformation. However, due to the decreasing time scale available for strain accommodation restricted by the increasing loading rate, the complement of dislocations movement is getting more difficult at higher loading rates and more “delayed plasticity” would be accumulated. Upon the commence of the creep stage, the delayed dislocation movements take place and higher loading rates are expected to lead to more significant creep depth.

Here, our results provide an alternative understanding that the restricted time scale available for dislocation movements might not be the main cause. As shown in Fig. 6 (b), for the crystallized MGs, with the loading rate increasing from 0.33 mN/s to 70 mN/s, the relaxation time decreases from ~10s to ~0.1s, indicating that the deformation accommodation rate increases accordingly along with the loading rate. This result suggests that the loading rate might not beat the slide velocity of the dislocations. The decreasing serrations of the crystallized Pd MG in Fig. 4(b) also support the sufficient deformation accommodation rate in the loading stage, as interpreted in **Part 4.1**.

Based on our results, as illustrated in Fig. 10 (a) and (b), the increasing creep depth is probably due to the enhanced collective

mode in the operation of dislocations. Larger numbers of dislocations or STZs operates synchronically would naturally lead to a higher creep depth in the creep stage as shown in Fig. 5. The increasing tendency of the collective movements of dislocations or STZs has already been demonstrated by the stretched exponent β in Fig. 6(a). From this kinematic perspective, the softening effect in the MGs is also probably resulted from the collective mode in the activation dynamics of elementary deformation units.

5. Conclusions

To conclude, nanoindentation on 3 MGs in both crystallized and glassy states are conducted in a range of loading rates from 0.33 mN/s to 70 mN/s. The deformation behaviors in the creep stage of nanoindentation of both the glassy and crystallized MGs are characterized with the Kohlrausch-Williams-Watts (KWW) equation to exhibit similar softening phenomena. The stretched exponent and relaxation time indicate the homological softening dynamics in the plastic deformation of the MGs both in glassy and crystallized states. Especially, the relaxation time of the glassy La MG precludes the possibility of shear dilatation being the main cause for the softening of the glassy MGs. For the distinct elementary deformation units and noting the absence of dilatation in dislocations, the softening in the plastic deformation of the glassy and crystallized MGs is thus suggested to originate from the collective mode in the activation dynamics of the elementary deformation units (STZs in glassy MGs and dislocations in crystallized MGs). The relaxation time of the glassy MGs is intimately related to JG relaxation, whilst that the underlying physics requires further clarification. More works on the creep stage of nanoindentation on MGs would advance current knowledges on the plasticity mechanisms and the nature of structural relaxation in MGs.

Acknowledgements

This work was financially supported by the National Nature and Science Foundation of China under grant No. 51701082, “the Fundamental Research Funds for the Central Universities” and the Guangdong Province Science and Technology Plan under grant No. 2017B090903005. M.Z. and Y.C. are also grateful for the support of the Opening Fund of State Key Laboratory of Non-linear Mechanics(No. LNM201812).

References

Afonin, G.V., Mitrofanov, Y.P., Makarov, A.S., Kobelev, N.P., Wang, W.H., Khonik, V.A., 2016. Universal relationship between crystallization-induced changes of the shear modulus and heat release in metallic glasses. Acta Mater. 115, 204–209.
Argon, A.S., 1979. Plastic deformation in metallic glasses. Acta Metall. 27, 47–58.
Bhowmick, R., Raghavan, R., Chattopadhyay, K., Ramamurty, U., 2006. Plastic flow softening in a bulk metallic glass. Acta Mater. 54, 4221–4228.
Burgess, T., Ferry, M., 2009. Nanoindentation of metallic glasses. Mater. Today 12, 24–32.
Castellero, A., Moser, B., Uhlenhaut, D.I., Dalla Torre, F.H., Loffler, J.F., 2008. Room-temperature creep and structural relaxation of Mg-Cu-Y metallic glasses. Acta Mater. 56, 3777–3785.
Chattoraj, J., Lemaitre, A., 2013. Elastic signature of flow events in supercooled liquids under shear. Phys. Rev. Lett. 111 066001.
Chen, J., Shen, Y.F., Liu, W.L., Beake, B.D., Shi, X.R., Wang, Z.M., Zhang, Y., Guo, X.L., 2016. Effects of loading rate on development of pile-up during indentation creep of polycrystalline copper. Mater. Sci. Eng. A-Struct. Mater. Prop. Microstruct. Process. 656, 216–221.
Chen, K.W., Lin, J.F., 2010. Investigation of the relationship between primary and secondary shear bands induced by indentation in bulk metallic glasses. Int. J. Plast. 26, 1645–1658.
Chen, Y., Jiang, M.Q., Dai, L.H., 2013. Collective evolution dynamics of multiple shear bands in bulk metallic glasses. Int. J. Plast. 50, 18–36.
Cheng, Y.Q., Ma, E., 2011. Atomic-level structure and structure–property relationship in metallic glasses. Prog. Mater. Sci. 56, 379–473.
Dahlberg, C.V.O., Saito, Y., Oztop, M.S., Kysar, J.W., 2014. Geometrically necessary dislocation density measurements associated with different angles of indentations. Int. J. Plast. 54, 81–95.
Dean, J., Wheeler, J.M., Clyne, T.W., 2010. Use of quasi-static nanoindentation data to obtain stress strain characteristics for metallic materials. Acta Mater. 58, 3613–3623.
Ding, J., Cheng, Y.Q., Sheng, H., Asta, M., Ritchie, R.O., Ma, E., 2016. Universal structural parameter to quantitatively predict metallic glass properties. Nat. Commun. 7 13733.
Fornell, J., Concustell, A., Surinach, S., Li, W.H., Cuadrado, N., Gebert, A., Baro, M.D., Sort, J., 2009. Yielding and intrinsic plasticity of Ti-Zr-Ni-Cu-Be bulk metallic glass. Int. J. Plast. 25, 1540–1559.
Gan, M., Tomar, V., 2010. Role of length scale and temperature in indentation induced creep behavior of polymer derived Si-C-O ceramics. Mater. Sci. Eng. A-Struct. Mater. Prop. Microstruct. Process. 527, 7615–7623.
Gerberich, W., Venkataraman, S., Huang, H., Harvey, S., Kohlstedt, D., 1995. The injection of plasticity by millinewton contacts. Acta Metall. Mater. 43, 1569–1576.
Ginder, R.S., Nix, W.D., Pharr, G.M., 2018. A simple model for indentation creep. J. Mech. Phys. Solid. 112, 552–562.
Haghshenas, M., Wang, Y., Cheng, Y.T., Gupta, M., 2018. Indentation-based rate-dependent plastic deformation of polycrystalline pure magnesium. Mater. Sci. Eng. A-Struct. Mater. Prop. Microstruct. Process. 716, 63–71.
Harmon, J.S., Demetriou, M.D., Johnson, W.L., Samwer, K., 2007. Anelastic to plastic transition in metallic glass-forming liquids. Phys. Rev. Lett. 99 135502.
Hufnagel, T.C., Schuh, C.A., Falk, M.L., 2016. Deformation of metallic glasses: recent developments in theory, simulations, and experiments. Acta Mater. 109, 375–393.
Jang, D.C., Gross, C.T., Greer, J.R., 2011. Effects of size on the strength and deformation mechanism in Zr-based metallic glasses. Int. J. Plast. 27, 858–867.
Jiang, M.Q., Dai, L.H., 2009. On the origin of shear banding instability in metallic glasses. J. Mech. Phys. Solid. 57, 1267–1292.
Jiang, M.Q., Peterlechner, M., Wang, Y.J., Wang, W.H., Jiang, F., Dai, L.H., Wilde, G., 2017. Universal structural softening in metallic glasses indicated by boson heat capacity peak. Appl. Phys. Lett. 111 261901.
Ketov, S.V., Sun, Y.H., Nachum, S., Lu, Z., Checchi, A., Beraldin, A.R., Bai, H.Y., Wang, W.H., Louzguine-Luzgin, D.V., Carpenter, M.A., Greer, A.L., 2015. Rejuvenation of metallic glasses by non-affine thermal strain. Nature 524, 200.
Khan, M.M., Nemati, A., Rahman, Z.U., Shah, U.H., Asgar, H., Haider, W., 2018. Recent advancements in bulk metallic glasses and their applications: a review. Crit. Rev. Solid State Mater. Sci. 43, 233–268.
Klaumünzer, D., Maaß, R., Löffler, J.F., 2011. Stick-slip dynamics and recent insights into shear banding in metallic glasses. J. Mater. Res. 26, 1453–1463.
Kramer, L., Maier-Kiener, V., Champion, Y., Sarac, B., Pippan, R., 2018. Activation volume and energy of bulk metallic glasses determined by nanoindentation. Mater. Des. 155, 116–124.
Lee, D.H., Seok, M.Y., Zhao, Y., Choi, I.C., He, J., Lu, Z.P., Suh, J.Y., Ramamurty, U., Kawasaki, M., Langdon, T.G., Jang, J.I., 2016. Spherical nanoindentation creep behavior of nanocrystalline and coarse-grained CoCrFeMnNi high-entropy alloys. Acta Mater. 109, 314–322.
Li, H.F., Zheng, Y.F., 2016. Recent advances in bulk metallic glasses for biomedical applications. Acta Biomater. 36, 1–20.

Liu, E.Q., Wang, H.F., Xiao, G.S., Yuan, G.Z., Shu, X.F., 2015. Creep-related micromechanical behavior of zirconia-based ceramics investigated by nanoindentation. Ceram. Int. 41, 12939–12944.
Lu, Y.Z., Jiang, M.Q., Lu, X., Qin, Z.X., Huang, Y.J., Shen, J., 2018. Dilatancy of shear transformations in a colloidal glass. Phys. Rev. Appl. 9 014023.
Luttich, M., Giordano, V.M., Le Floch, S., Pineda, E., Zontone, F., Luo, Y.S., Samwer, K., Ruta, B., 2018. Anti-aging in ultrastable metallic glasses. Phys. Rev. Lett. 120 135504.
Ma, Z.S., Zhou, Y.C., Long, S.G., Lu, C., 2012. On the intrinsic hardness of a metallic film/substrate system: indentation size and substrate effects. Int. J. Plast. 34, 1–11.
Mahjoub, R., Hamilton, N.E., Laws, K.J., Ferry, M., 2016. Softening of phonon spectra in metallic glasses. NPJ Comput. Mater. 2 16029.
Maier, V., Merle, B., Goken, M., Durst, K., 2013. An improved long-term nanoindentation creep testing approach for studying the local deformation processes in nanocrystalline metals at room and elevated temperatures. J. Mater. Res. 28, 1177–1188.
Murali, P., Ramamurty, U., Shenoy, V.B., 2007. Strain accommodation in inelastic deformation of glasses. Phys. Rev. B 75 024203.
Oliver, W.C., Pharr, G.M., 2010. Nanoindentation in materials research: past, present, and future. MRS Bull. 35, 897–907.
Pan, J., Chen, Q., Liu, L., Li, Y., 2011. Softening and dilatation in a single shear band. Acta Mater. 59, 5146–5158.
Pan, J., Wang, Y.X., Guo, Q., Zhang, D., Greer, A.L., Li, Y., 2018. Extreme rejuvenation and softening in a bulk metallic glass. Nat. Commun. 9, 560.
Patinet, S., Vandembroucq, D., Falk, M.L., 2016. Connecting local yield stresses with plastic activity in amorphous solids. Phys. Rev. Lett. 117 045501.
Phani, P.S., Oliver, W.C., 2016. A direct comparison of high temperature nanoindentation creep and uniaxial creep measurements for commercial purity aluminum. Acta Mater. 111, 31–38.
Qiao, J.C., Pelletier, J.M., 2014. Dynamic mechanical relaxation in bulk metallic glasses: a review. J. Mater. Sci. Technol. 30, 523–545.
Qiao, J.C., Yao, Y., Pelletier, J.M., Keer, L.M., 2016. Understanding of micro-alloying on plasticity in Cu46Zr47-xAl7Dyx (0 < = x < = 8) bulk metallic glasses under compression: based on mechanical relaxations and theoretical analysis. Int. J. Plast. 82, 62–75.
Schmidt, V., Rosner, H., Peterlechner, M., Wilde, G., 2015. Quantitative measurement of density in a shear band of metallic glass monitored along its propagation direction. Phys. Rev. Lett. 115 035501.
Schuh, C.A., Lund, A.C., Nieh, T.G., 2004. New regime of homogeneous flow in the deformation map of metallic glasses: elevated temperature nanoindentation experiments and mechanistic modeling. Acta Mater. 52, 5879–5891.
Schuh, C.A., Nieh, T.G., 2003. A nanoindentation study of serrated flow in bulk metallic glasses. Acta Mater. 51, 87–99.
Schuh, C.A., Nieh, T.G., 2004. A survey of instrumented indentation studies on metallic glasses. J. Mater. Res. 19, 46–57.
Schuh, C.A., Nieh, T.G., Kawamura, Y., 2002. Rate dependence of serrated flow during nanoindentation of a bulk metallic glass. J. Mater. Res. 17, 1651–1654.
Selyutina, N., Borodin, E.N., Petrov, Y., Mayer, A.E., 2016. The definition of characteristic times of plastic relaxation by dislocation slip and grain boundary sliding in copper and nickel. Int. J. Plast. 82, 97–111.
Sneddon, I.N., 1965. The relation between load and penetration in the axisymmetric boussinesq problem for a punch of arbitrary profile. Int. J. Eng. Sci. 3, 47–57.
Sopu, D., Stukowski, A., Stoica, M., Scudino, S., 2017. Atomic-Level processes of shear band nucleation in metallic glasses. Phys. Rev. Lett. 119 195503.
Spaepen, F., 1977. A microscopic mechanism for steady state inhomogeneous flow in metallic glasses. Acta Metall. 25, 407–415.
Su, C.J., Herbert, E.G., Sohn, S., LaManna, J.A., Oliver, W.C., Pharr, G.M., 2013. Measurement of power-law creep parameters by instrumented indentation methods. J. Mech. Phys. Solid. 61, 517–536.
Su, C.J., LaManna, J.A., Gao, Y.F., Oliver, W.C., Pharr, G.M., 2010. Plastic instability in amorphous selenium near its glass transition temperature. J. Mater. Res. 25, 1015–1019.
Tehrani, M., Safdari, M., Al-Haik, M.S., 2011. Nanocharacterization of creep behavior of multiwall carbon nanotubes/epoxy nanocomposite. Int. J. Plast. 27, 887–901.
Wang, C.L., Lai, Y.H., Huang, J.C., Nieh, T.G., 2010. Creep of nanocrystalline nickel: a direct comparison between uniaxial and nanoindentation creep. Scripta Mater. 62, 175–178.
Wang, P., Liu, F.X., Cui, Y.A., Liu, Z.L., Qu, S.X., Zhuang, Z., 2018a. Interpreting strain burst in micropillar compression through instability of loading system. Int. J. Plast. 107, 150–163.
Wang, Q., Liu, J.J., Ye, Y.F., Liu, T.T., Wang, S., Liu, C.T., Lu, J., Yang, Y., 2017. Universal secondary relaxation and unusual brittle-to-ductile transition in metallic glasses. Mater. Today 20, 293–300.
Wang, W.H., 2009. Bulk metallic glasses with functional physical properties. Adv. Mater. 21, 4524–4544.
Wang, Y.-J., Ishii, A., Ogata, S., 2013. Entropic effect on creep in nanocrystalline metals. Acta Mater. 61, 3866–3871.
Wang, Y.J., Zhang, M., Liu, L., Ogata, S., Dai, L.H., 2015. Universal enthalpy-entropy compensation rule for the deformation of metallic glasses. Phys. Rev. B 92 174118.
Wang, Y.Q., Zhang, J.J., Wu, K., Liu, G., Kiener, D., Sun, J., 2018b. Nanoindentation creep behavior of Cu-Zr metallic glass films. Mater. Res. Lett. 6, 22–28.
Wang, Z., Sun, B.A., Bai, H.Y., Wang, W.H., 2014. Evolution of hidden localized flow during glass-to-liquid transition in metallic glass. Nat. Commun. 5, 5823.
Wei, B.C., Zhang, L.C., Zhang, T.H., Xing, D.M., Das, J., Eckert, J., 2007. Strain rate dependence of plastic flow in Ce-based bulk metallic glass during nanoindentation. J. Mater. Res. 22, 258–263.
Williams, G., Watts, D.C., 1970. Non-symmetrical dielectric relaxation behaviour arising from a simple empirical decay function. Trans. Faraday Soc. 66, 80–85.
Wu, F.F., Zheng, W., Wu, S.D., Zhang, Z.F., Shen, J., 2011. Shear stability of metallic glasses. Int. J. Plast. 27, 560–575.
Wu, Y., Bei, H., Wang, Y.L., Lu, Z.P., George, E.P., Gao, Y.F., 2015. Deformation-induced spatiotemporal fluctuation, evolution and localization of strain fields in a bulk metallic glass. Int. J. Plast. 71, 136–145.
Wu, Y., Wu, H.H., Hui, X.D., Chen, G.L., Lu, Z.P., 2010. Effects of drawing on the tensile fracture strength and its reliability of small-sized metallic glasses. Acta Mater. 58, 2564–2576.
Xiao, X.Z., Terentyev, D., Chen, Q.Y., Yu, L., Chen, L.R., Bakaev, A., Duan, H.L., 2017. The depth dependent hardness of bicrystals with dislocation transmission through grain boundaries: a theoretical model. Int. J. Plast. 90, 212–230.
Yang, X.N., Liu, R., Yang, M.C., Wang, W.H., Chen, K., 2016a. Structures of local rearrangements in soft colloidal glasses. Phys. Rev. Lett. 116 238003.
Yang, Y.J., Luo, J., Huang, L.P., Hu, G.L., Vargheese, K.D., Shi, Y.F., Mauro, J.C., 2016b. Crack initiation in metallic glasses under nanoindentation. Acta Mater. 115, 413–422.
Yoo, B.G., Kim, J.Y., Kim, Y.J., Choi, I.C., Shim, S., Tsui, T.Y., Bei, H.B., Ramamurty, U., Jang, J.I., 2012. Increased time-dependent room temperature plasticity in metallic glass nanopillars and its size-dependency. Int. J. Plast. 37, 108–118.
Yu, H.B., Shen, X., Wang, Z., Gu, L., Wang, W.H., Bai, H.Y., 2012. Tensile plasticity in metallic glasses with pronounced β relaxations. Phys. Rev. Lett. 108 015504.
Yu, H.B., Wang, W.H., Bai, H.Y., Samwer, K., 2014. The beta-relaxation in metallic glasses. Natl. Sci. Rev. 1, 429–461.
Zaiser, M., Hahner, P., 1997. Oscillatory modes of plastic deformation: theoretical concepts. Phys. Status Solidi B-Basic Res. 199, 267–330.
Zhang, L., Ohmura, T., 2014. Plasticity initiation and evolution during nanoindentation of an iron-3% silicon crystal. Phys. Rev. Lett. 112, 5.
Zhang, L.J., Yu, P.F., Cheng, H., Zhang, H., Diao, H.Y., Shi, Y.Z., Chen, B.L., Chen, P.Y., Feng, R., Bai, J., Jing, Q., Ma, M.Z., Liaw, P.K., Li, G., Liu, R.P., 2016a. Nanoindentation creep behavior of an Al0.3CoCrFeNi high-entropy alloy. Metall. Mater. Trans. A-Phys. Metall. Mater. Sci. 47A, 5871–5875.
Zhang, M., Chen, Y., Wei, D., Dai, L.H., 2018. Extraordinary creep relaxation time in a La-based metallic glass. J. Mater. Sci. 53, 2956–2964.
Zhang, M., Liu, L., Wu, Y., 2013. Facilitation and correlation of flow in metallic supercooled liquid. J. Chem. Phys. 139 164508.
Zhang, M., Wang, Y.J., Dai, L.H., 2016b. Understanding the serrated flow and Johari-Goldstein relaxation of metallic glasses. J. Non-Cryst. Solids 444, 23–30.
Zhang, W., Gao, Y.F., Xia, Y.Z., Bei, H.B., 2017a. Indentation Schmid factor and incipient plasticity by nanoindentation pop-in tests in hexagonal close-packed single crystals. Acta Mater. 134, 53–65.
Zhang, Y., Mohanty, D.P., Seiler, P., Siegmund, T., Kruzic, J.J., Tomar, V., 2017b. High temperature indentation based property measurements of IN-617. Int. J. Plast. 96, 264–281.
Zylberg, J., Lerner, E., Bar-Sinai, Y., Bouchbinder, E., 2017. Local thermal energy as a structural indicator in glasses. Proc. Natl. Acad. Sci. U. S. A 114, 7289–7294.